

Interaction of Mechanical Oscillators Mediated by the Exchange of Virtual Photon Pairs

Omar Di Stefano,¹ Vincenzo Macrì,^{1,2} Alessandro Ridolfo,¹ Roberto Stassi,¹ Anton Frisk Kockum,¹ Salvatore Savasta,^{1,2,*} and Franco Nori^{1,3}

¹*Center for Emergent Matter Science, RIKEN, Saitama 351-0198, Japan*

²*Dipartimento di Scienze Matematiche e Informatiche,*

Scienze Fisiche e Scienze della Terra, Università di Messina, I-98166 Messina, Italy

³*Physics Department, The University of Michigan, Ann Arbor, Michigan 48109-1040, USA*

Two close parallel mirrors attract due to a small force (Casimir effect) originating from the electromagnetic quantum vacuum fluctuations of the electromagnetic field. These vacuum fluctuations can also induce motional forces exerted upon one mirror when the other one moves. Here we consider an optomechanical system consisting of two vibrating mirrors coupled to an optical resonator. We find that motional forces can determine noticeable coupling rates between the two spatially separated vibrating mirrors. We show that, by tuning the two mechanical oscillators into resonance, energy is exchanged between them at the quantum level. This coherent motional coupling is enabled by the exchange of virtual photon pairs, originating from the dynamical Casimir effect. The process proposed here shows that the electromagnetic quantum vacuum is able to transfer mechanical energy somewhat like an ordinary fluid. We show that this system can also operate as a mechanical parametric down-converter even at very weak excitations. These results demonstrate that vacuum-induced motional forces open up new possibilities for the development of optomechanical quantum technologies.

Effective interactions able to coherently couple spatially separated qubits [1] are highly desirable for any quantum computer architecture. Efficient cavity-QED schemes, where the effective long-range interaction is mediated by the vacuum field, have been proposed [2–4] and realized [1, 5, 6]. In these schemes, the cavity is only virtually excited and thus the requirement on its quality factor is greatly loosened. Based on these interactions mediated by vacuum fluctuations, a two-qubit gate has been realized [7] and two-qubit entanglement has been demonstrated [1]. Creation of multi-qubit entanglement [8] has also been demonstrated in circuit-QED systems. Very recently, it has been shown that the exchange of virtual photons between artificial atoms can give rise to effective interactions of multiple spatially-separated atoms [9, 10], opening the way to vacuum nonlinear optics. Moreover, it has been shown that systems where virtual photons can be created and annihilated can be used to realize many nonlinear optical processes with qubits [11, 12]. Multiparticle entanglement and quantum logic gates, via virtual vibrational excitations in an ion trap, have also been implemented [13, 14].

Given these results, one may wonder whether it is possible for spatially separated mesoscopic or macroscopic bodies to interact at a quantum level by means of the vacuum fluctuations of the electromagnetic field. It is known that, owing to quantum fluctuations, the electromagnetic vacuum is able, in principle, to affect the motion of objects through it, like a complex fluid [15]. For example, it can induce dissipation and decoherence effects on the motion of moving objects [16, 17]. By using linear dispersion theory, it has also been shown that vacuum fluctuations can induce motional forces exerted

upon one mirror when the other one moves [18]. Here we show that two spatially separated moveable mirrors, constituting a cavity-optomechanical system, can exchange energy coherently and reversibly, by exchanging virtual photon pairs. The effects described here can be experimentally demonstrated with circuit-optomechanical systems, using ultra-high-frequency mechanical micro- or nano-resonators in the GHz spectral range [19, 20]. A great advantage of high-frequency mechanical oscillators is that they can be cooled to their ground state by using conventional cryogenic refrigeration [19]. Coupling such a mechanical oscillator to a superconducting qubit, quantum control over a macroscopic mechanical system has been demonstrated [19].

Our results show that the electromagnetic quantum vacuum is able to transfer mechanical energy somewhat like an ordinary fluid. It would be as if the vibration of a string (mechanical oscillator 1) could be transferred to the membrane of a microphone (mechanical oscillator 2) in the absence of air (or any excited medium filling the gap).

We consider a system constituted by two vibrating mirrors interacting via radiation pressure [see Fig. 1(a)]. Very recently, entanglement between two mechanical oscillators has been demonstrated in a similar system, where, however, the two entangled mechanical oscillators have much lower resonance frequencies and the system is optically pumped [21]. This system can be described by a Hamiltonian that is a direct generalization to two mirrors of the Law Hamiltonian, describing the coupled mirror-field system [22–24]. It provides a unified description of cavity-optomechanics experiments [25] and of the dynamical Casimir effect (DCE) [26–30] in a cavity with a

vibrating mirror [23]. It has been shown [28–34] that the photon pairs generated by the DCE can be used to produce entanglement. However, in the present case, the interaction and the entanglement between two mechanical oscillators is determined by virtual photon pairs. Both the cavity field and the position of the mirror are treated as dynamical variables and a canonical quantization procedure is adopted [22]. By considering only one mechanical mode for each mirror, with resonance frequency ω_i ($i = 1, 2$) and bosonic operators \hat{b}_i and \hat{b}_i^\dagger , the displacement operators can be expressed as $\hat{x}_i = X_{\text{zpf}}^{(i)}(\hat{b}_i^\dagger + \hat{b}_i)$, where $X_{\text{zpf}}^{(i)}$ is the zero-point-fluctuation amplitude of the i th mirror. The mirrors form a single-mode optical resonator with frequency ω_c and bosonic photon operators \hat{a} and \hat{a}^\dagger . The system Hamiltonian can be written as $\hat{H}_s = \hat{H}_0 + \hat{H}_I$, where ($\hbar = 1$) $\hat{H}_0 = \omega_c \hat{a}^\dagger \hat{a} + \sum_i \omega_i \hat{b}_i^\dagger \hat{b}_i$ is the unperturbed Hamiltonian. The mirror-field interaction Hamiltonian can be written as $\hat{H}_I = \hat{V}_{\text{om}} + \hat{V}_{\text{DCE}}$, where $\hat{V}_{\text{om}} = \hat{a}^\dagger \hat{a} \sum_i g_i (\hat{b}_i + \hat{b}_i^\dagger)$ is the standard optomechanical interaction conserving the number of photons, $\hat{V}_{\text{DCE}} = (1/2)(\hat{a}^2 + \hat{a}^{\dagger 2}) \sum_i g_i (\hat{b}_i + \hat{b}_i^\dagger)$ describes the creation and annihilation of photon pairs, and g_i is the optomechanical coupling rate for mirror i . The linear dependence of the interaction Hamiltonian on the mirror operators is a consequence of the usual small-displacement assumption [22]. This Hamiltonian can be directly generalized to include additional cavity modes. However, in most circuit-optomechanics experiments, the electromagnetic resonator is provided by a superconducting LC circuit, which only supports a *single* mode.

When describing most of the optomechanics experiments to date [25], \hat{V}_{DCE} is neglected. This is a very good approximation when $\omega_i \ll \omega_c$ (which is the most common experimental situation). However, when ω_i are of the order of ω_c , \hat{V}_{DCE} cannot be neglected. We are interested in studying this regime, which can be achieved using microwave resonators and ultra-high-frequency mechanical micro- or nano-resonators [19, 20]. The Hamiltonian \hat{H}_s describes the interaction between two vibrating mirrors and the radiation pressure of a cavity field. However, the same radiation-pressure-type coupling is obtained for microwave optomechanical circuits (see, e.g., Ref. [35]).

In order to properly describe the system dynamics, including external driving and dissipation, the coupling to external degrees of freedom needs to be considered. A coherent external drive of the vibrating mirror i can be described by including the time-dependent Hamiltonian

$$\hat{V}_i(t) = \mathcal{F}_i(t) (\hat{b}_i + \hat{b}_i^\dagger), \quad (1)$$

where $\mathcal{F}_i(t)$ is equal to the external force applied to the mirror times the mechanical zero-point-fluctuation amplitude. Dissipation and decoherence effects are taken into account by adopting a master-equation approach. For strongly coupled hybrid quantum systems, the description offered by the standard quantum-optical master

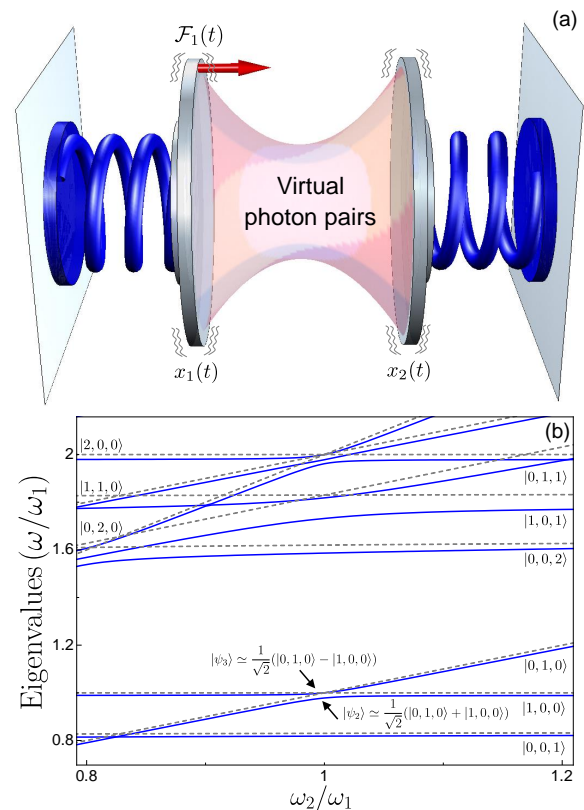


Figure 1. (a) Schematic of an optomechanical system constituted by two vibrating mirrors. If one of the two vibrating mirrors is excited by an external drive $\mathcal{F}_1(t)$, its excitation can be transferred coherently and reversibly to the other mirror. The interaction is mediated by the exchange of virtual photon pairs. (b) Lowest energy levels of the system Hamiltonian as a function of the ratio between the mechanical frequency of mirror 2 and that of mirror 1. An optomechanical coupling $g/\omega_1 = 0.1$ has been used; the cavity-mode resonance frequency is $\omega_c = 0.85\omega_1$. The clearly visible anticrossings are the signature of the mirror-mirror interaction mediated by the virtual DCE photons.

equation breaks down [36, 37]. Following Refs. [37–39], we express the system-bath interaction Hamiltonian in the basis formed by the energy eigenstates of \hat{H}_s [23]. Throughout this letter we assume a zero-temperature reservoir.

We begin our analysis by numerically diagonalizing the Hamiltonian H_s in a truncated finite-dimensional Hilbert space. The truncation is realized by only including the lowest-energy N_c photonic and N_1, N_2 mechanical Fock states. These truncation numbers are chosen in order to ensure that the lowest $M < N_c \times N_1 \times N_2$ energy eigenvalues and the corresponding eigenvectors, which are involved in the dynamical processes investigated here, are not significantly affected when increasing N_c and N_i ($i = 1, 2$).

The blue solid curves in Fig. 1(b) describe the eigenvalue differences $E_j - E_0$ (E_0 is the ground-state energy)

of the total Hamiltonian \hat{H}_s (including \hat{V}_{DCE}) as a function of ω_2/ω_1 . For the optomechanical couplings, we use $g_1 = g_2 = g = 0.1\omega_1$. Such a coupling strength is at the onset of the so-called ultrastrong optomechanical coupling regime [37, 40, 41]. The cavity-mode resonance frequency is fixed at $\omega_c = 0.85\omega_1$. This value is chosen such that the resonance condition for the DCE [23] $2\omega_c \approx k_1\omega_1 + k_2\omega_2$ is *not* fulfilled. For comparison, we also show in Fig. 1(b) (dashed grey lines) the lowest energy levels $E_{n,k_1,k_2} = \omega_c n - \sum_i g_i^2 n^2 / \omega_i + \sum_i \omega_i k_i$ of the standard optomechanics Hamiltonian $\hat{H}_0 + \hat{V}_{\text{om}}$. This Hamiltonian has the eigenstates $|k_1, k_2, n\rangle \equiv D_1(n\beta_1)|k\rangle_1 \otimes D_2(n\beta_2)|k\rangle_2 \otimes |n\rangle_c$, where $|n\rangle_c$ is the cavity Fock state and $|k\rangle_i$ is the bare mechanical state for the i th mirror.

The bare mechanical states $|k\rangle_i$ are displaced by the optomechanical interaction, $\hat{D}_i(n\beta_i) = \exp[n\beta_i(\hat{b}_i^\dagger - \hat{b}_i)]$, with $\beta_i = g_i/\omega_i$ (see Sec. I of Supplemental Material [42]). The main differences between the blue solid and the grey dashed curves are the appearance of small energy shifts, and of level anticrossings in the region $\omega_2/\omega_1 \sim 1$. We indicate by $|\psi_n\rangle$ ($n = 0, 1, 2 \dots$) the eigenvectors of \hat{H}_s and by E_n the corresponding eigenvalues, choosing the labeling of the states such that $E_j > E_k$ for $j > k$. Starting from the lowest energy levels, we first meet a splitting originating from the coherent coupling of the zero-photon states $|1, 0, 0\rangle$ and $|0, 1, 0\rangle$. At the minimum energy splitting, the resulting states are well approximated by $|\psi_{2,3}\rangle \simeq (1/\sqrt{2})(|1, 0, 0\rangle \pm |0, 1, 0\rangle)$. As we will show explicitly below by using perturbation theory, this *mirror-mirror interaction is a result of virtual exchange of cavity photon pairs*. When the mirrors have the same resonance frequency, an excitation in one mirror can be transferred to the other by virtually becoming a photon pair in the cavity, thanks to the DCE. This coherent coupling is greatly enhanced by the presence of a cavity photon, resulting in the larger splitting ($E_6 - E_5$), corresponding to the states $|\psi_{5,6}\rangle \simeq (1/\sqrt{2})(|1, 0, 1\rangle \pm |0, 1, 1\rangle)$. At higher energy, at $\omega_2/\omega_1 \sim 1$, \hat{V}_{DCE} removes the degeneracy between the three states $|2, 0, 0\rangle$, $|0, 2, 0\rangle$, and $|1, 1, 0\rangle$, determining a two-phonon coupling between the two mirrors.

The origin of the avoided-level crossings shown in Fig. 1(b) can be understood by deriving an effective Hamiltonian, using second-order perturbation theory or, equivalently, the James' method [43, 44] (see Sec. II in [42]). The resulting effective Hamiltonian, describing the coherent coupling of states $|1, 0, 0\rangle$ and $|0, 1, 0\rangle$, is

$$\hat{H}_{\text{eff}} = \Omega_1|1, 0, 0\rangle\langle 1, 0, 0| + \Omega_2|0, 1, 0\rangle\langle 0, 1, 0| + (\lambda_{10}^{01}|1, 0, 0\rangle\langle 0, 1, 0| + \text{H.c.}), \quad (2)$$

where $\Omega_1 = \omega_1 + \Delta_{10}$ and $\Omega_2 = \omega_2 + \Delta_{01}$ denote the Lamb-shifted levels [42]. The effective coupling strength is

$$\lambda_{10}^{01} = \sum_{k,q} \frac{\langle 0, 1, 0 | \hat{V}_{\text{DCE}} | k, q, 2 \rangle \langle k, q, 2 | \hat{V}_{\text{DCE}} | 1, 0, 0 \rangle}{E_{0,1,0} - E_{2,k,q}}. \quad (3)$$

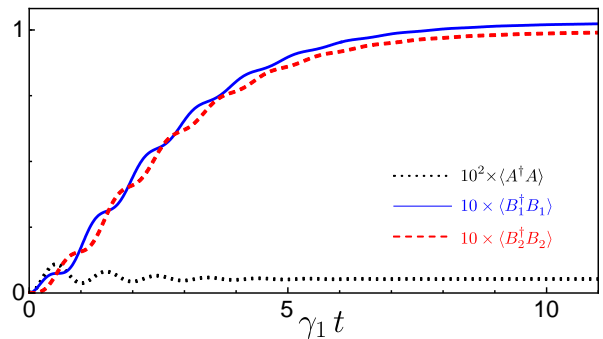


Figure 2. System dynamics for $\omega_c \simeq 1.5\omega_1$ under continuous-wave drive of mirror 1. The blue solid and red dashed curves describe the mean phonon numbers $\langle \hat{B}_1^\dagger \hat{B}_1 \rangle$ and $\langle \hat{B}_2^\dagger \hat{B}_2 \rangle$, respectively, while the black dotted curve describes the mean intracavity photon number $\langle \hat{A}^\dagger \hat{A} \rangle$ arising due to the DCE.

Equations (2) and (3) clearly show that the one-phonon state of mirror 1 can be transferred to mirror 2 through a virtual transition via the two-photon intermediate states $|k, q, 2\rangle$. We notice that the largest contribution is provided by the zero-photon intermediate state ($k = q = 0$). This perturbative calculation gives rise to an effective coupling strength λ and energy shifts Δ in good agreement with the numerical calculation shown in Fig. 1(b) (see Sec. III of [42]). Analogous effective Hamiltonians can be derived for the avoided-level crossings at higher energy (see Sec. III of [42]).

If the optomechanical couplings g_i are strong enough to ensure that the DCE-induced effective coupling (3) becomes larger than the relevant decoherence rates in the system, the transfer of one-phonon excitations between the two mirrors can be deterministic and reversible. Neglecting decoherence (calculations including losses can be found in Secs. IV and V of [42]), if the system is initially prepared in the state $|1, 0, 0\rangle$, it will evolve as

$$|\psi(t)\rangle = \cos(\lambda_{10}^{01}t)|1, 0, 0\rangle - i \sin(\lambda_{10}^{01}t)|0, 1, 0\rangle. \quad (4)$$

After a time $t = \pi/(2\lambda_{10}^{01})$, the excitation will be completely transferred to mirror 1. After a time $t = \pi/(4\lambda_{10}^{01})$, the two mirrors will be in a maximally entangled motional state.

We investigate the system dynamics starting from its ground state and introducing the excitation of mirror 1 by a single-tone continuous-wave mechanical drive $\mathcal{F}_1(t) = \mathcal{A} \cos(\omega_1 t)$. Figure 2 shows the time evolution of the mean phonon numbers of the two mirrors $\langle \hat{B}_i^\dagger \hat{B}_i \rangle$ and the intracavity mean photon number $\langle \hat{A}^\dagger \hat{A} \rangle$. Here \hat{A}, \hat{B}_i are the *physical* photon and phonon operators. Such operators $\hat{O} = \hat{A}, \hat{B}_i$ can be defined in terms of their bare counterparts $\hat{o} = \hat{a}, \hat{b}_i$ as [45]

$$\hat{O} = \sum_{E_n > E_m} \langle \psi_m | (\hat{o} + \hat{o}^\dagger) | \psi_n \rangle | \psi_m \rangle \langle \psi_n |. \quad (5)$$

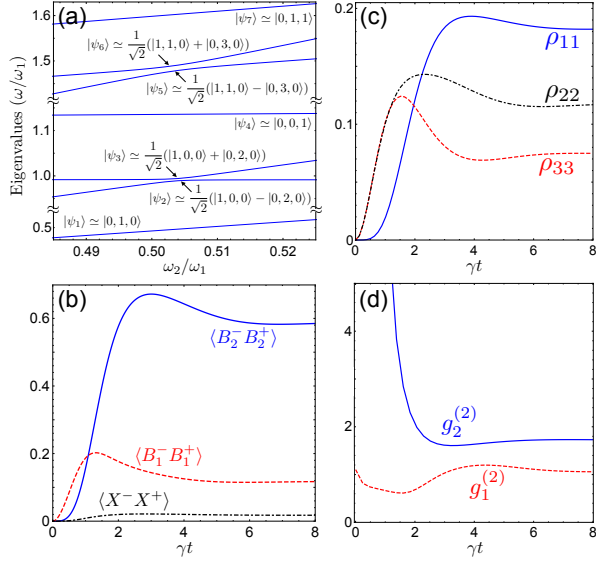


Figure 3. Mechanical parametric down-conversion. (a) Lowest energy levels of the system Hamiltonian as a function of the ratio between the mechanical frequency of mirror 2 and that of mirror 1. An optomechanical coupling $g/\omega_1 = 0.12$ has been used; the cavity-mode resonance frequency is $\omega_c = 1.2\omega_1$. Two avoided-level crossings are clearly visible. The one at lower energy corresponds to the resonant coupling of the one-phonon state of mirror 1 with the two-phonon state of mirror 2, whose resonance frequency is half that of mirror 1. The higher-energy anticrossing corresponds to the resonant coupling of the states $|1, 1, 0\rangle$ and $|0, 3, 0\rangle$. (b) Time evolution of the mean phonon and photon numbers. (c) Time evolution of the population of the first three energy states. (d) Equal-time phonon-phonon normalized correlation functions $g_i^{(2)}(t, t)$ for the two mirrors.

We assume a zero-temperature reservoir and use $\gamma_1 = \gamma_2 = \gamma = \omega_1/260$ and $\kappa = 2\gamma$ for the mechanical and photonic loss rates. We consider a weak ($\mathcal{A}/\gamma = 0.65$) resonant excitation of mirror 1 ($\omega_d = \omega_1$). We use a normalized coupling $g/\omega_1 = 0.1$, and we set $\omega_2 \simeq \omega_1$ at the value that provides the minimum level splitting $2\lambda_{10}^{01}$ [see Fig. 1(b)]. The results shown in Fig. 2 demonstrate that the excitation transfer mechanism via virtual DCE photon pairs, proposed here, works properly. In steady state, mirror 2 reaches almost the same excitation intensity as the driven mirror 1. The photon population remains very low throughout the considered time window.

In order to put forward the potentialities and the flexibility of this vacuum-field-mediated interaction between mechanical oscillators, we now show that this system also can operate as a mechanical parametric down-converter. For mechanical frequencies such that $\omega_1 \simeq 2\omega_2$, a ladder of avoided-level crossings manifests. Two of them are shown in Fig. 5(a). Also in this case, the avoided-level crossings originate from the exchange of virtual photon pairs, as can be understood by using second-order perturbation theory. For example, the dominant path for

the lowest energy level anticrossing goes through the intermediate state $|0, 0, 2\rangle$: $|1, 0, 0\rangle \leftrightarrow |0, 0, 2\rangle \leftrightarrow |0, 2, 0\rangle$ [42]. We note that these avoided-level crossings, in contrast to those shown in Fig. 5(a), do not conserve the excitation number. Analogous coherent coupling effects can be observed in the ultrastrong-coupling regime of cavity QED [9, 11, 39, 46, 47]. Using $\omega_c = 1.2\omega_1$ and $g/\omega_1 = 0.12$, we obtain a minimum energy splitting $\lambda_{10}^{02}/\omega_1 \simeq 4 \times 10^{-3}$. We fix the resonance frequency of mirror 2 at the value providing the minimum level splitting, and calculate the system dynamics considering a weak resonant excitation of mirror 1, $\mathcal{F}_1(t) = \mathcal{A} \cos(\omega_d t)$, with $\omega_d = (E_3 + E_2 - 2E_0)/2$, and $\mathcal{A}/\gamma = 0.7$. We also used $\gamma = 2 \times 10^{-3}\omega_1$ and $\kappa = \gamma/2$. The results shown in Fig. 5(b) demonstrate a very efficient excitation transfer between the two mechanical oscillators of different frequency. We also observe that the transfer occurs even in the presence of a very weak excitation of mirror 1 (peak mean phonon number of mirror 1: $\langle \hat{B}_1^\dagger \hat{B}_1 \rangle \simeq 0.2$). It may appear surprising that the steady-state mean phonon number of mirror 2 is significantly *larger* than that of mirror 1, even though it receives all the energy from the latter. This phenomenon can be partly understood by observing that a phonon of mirror 1 converts into two phonons (each at half energy) of mirror 2. In addition, once the system decays to the state $|\psi_1\rangle \simeq |0, 1, 0\rangle$, the remaining excitation in mirror 2 will not be exchanged back and forth with mirror 1, since the corresponding energy level is not resonantly coupled to other energy levels [see Fig. 5(a)]. Figure 5(c) displays the populations of the three lowest-energy levels, which are the levels that are most populated at this input power. This panel confirms that $|\psi_1\rangle$ has the higher population in steady state.

We also calculated the equal-time phonon-phonon normalized correlation functions

$$g_i^{(2)}(t, t) = \frac{\langle \hat{B}_i^\dagger(t) \hat{B}_i^\dagger(t) \hat{B}_i(t) \hat{B}_i(t) \rangle}{\langle \hat{B}_i^\dagger(t) \hat{B}_i(t) \rangle^2}. \quad (6)$$

The high value at early times obtained for mirror 2 [see Fig. 5(d)] confirms the *simultaneous excitation of phonon pairs*.

In conclusion, we demonstrated that mechanical quantum excitations can be coherently transferred among spatially-separated mechanical oscillators, through a dissipationless quantum bus, due to the exchange of virtual photon pairs. The experimental demonstration of these processes would show that the electromagnetic quantum vacuum is able to transfer mechanical energy somewhat like an ordinary fluid. The results presented here open up exciting possibilities of applying ideas from fluid dynamics in the study of the electromagnetic quantum vacuum. Furthermore, these results show that the DCE in high-frequency optomechanical systems can be a versatile and powerful new resource for the development of quantum

optomechanical technologies. If, in the future, it will be possible to control the interaction time (as currently realized in superconducting artificial atoms), e.g., changing rapidly the resonance frequencies of mechanical oscillators (see Sec. V of [42]), the interaction scheme proposed here would represent an attractive architecture for quantum information processing with optomechanical systems [48].

SUPPLEMENTAL MATERIAL

DIAGONALIZATION OF THE STANDARD OPTOMECHANICS HAMILTONIAN

We consider a system constituted by two vibrating mirrors interacting via radiation pressure [see Fig. 1(a) in the main paper]. Both the cavity field and the displacements of the mirrors are treated as dynamical variables and a canonical quantization procedure is adopted [22, 23].

By considering only one mechanical mode for each mirror, with resonance frequency ω_i ($i = 1, 2$) and bosonic operators \hat{b}_i and \hat{b}_i^\dagger , the displacement operators can be expressed as $\hat{x}_i = X_{\text{zpf}}^{(i)}(\hat{b}_i^\dagger + \hat{b}_i)$, where $X_{\text{zpf}}^{(i)}$ is the zero-point-fluctuation amplitude of the i th mirror. We also consider a single-mode optical resonator with frequency ω_c and bosonic photon operators \hat{a} and \hat{a}^\dagger . The system Hamiltonian can be written as $\hat{H}_s = \hat{H}_0 + \hat{H}_1$, where

$$\hat{H}_0 = \omega_c \hat{a}^\dagger \hat{a} + \omega_1 \hat{b}_1^\dagger \hat{b}_1 + \omega_2 \hat{b}_2^\dagger \hat{b}_2, \quad (7)$$

is the unperturbed Hamiltonian. The Hamiltonian describing the mirror-field interaction is

$$\hat{H}_1 = (\hat{a} + \hat{a}^\dagger)^2 \sum_{i=1,2} \frac{g_i}{2} (\hat{b}_i + \hat{b}_i^\dagger), \quad (8)$$

where g is the coupling rate. By developing the photonic operators in normal order, and by defining new bosonic phonon and photon operators and a renormalized photon frequency, \hat{H}_s can be written as

$$H_s = \hat{H}_{\text{om}} + \hat{V}_{\text{DCE}}, \quad (9)$$

where \hat{V}_{DCE} is the DCE interaction term:

$$\hat{V}_{\text{DCE}} = (\hat{a}^2 + \hat{a}^{\dagger 2}) \sum_{i=1,2} \frac{g_i}{2} (\hat{b}_i + \hat{b}_i^\dagger), \quad (10)$$

and \hat{H}_{om} is the standard optomechanics Hamiltonian:

$$\hat{H}_{\text{om}} = \hat{H}_0 + \hat{V}_{\text{om}} \quad (11)$$

with

$$\hat{V}_{\text{om}} = \hat{a}^\dagger \hat{a} \sum_{i=1,2} g_i (\hat{b}_i + \hat{b}_i^\dagger). \quad (12)$$

\hat{H}_{om} can be easily diagonalized defining the displacement operators for the two mirrors. In particular, defining ($i = 1, 2$)

$$\hat{B}_i = \hat{b}_i + \beta_i \hat{a}^\dagger \hat{a} \quad (13)$$

with $\beta_i = g_i/\omega_i$, we obtain

$$\begin{aligned} \hat{H}_{\text{om}} = \omega_c \left[1 - \left(\frac{\beta_1^2 \omega_1}{\omega_c} + \frac{\beta_2^2 \omega_2}{\omega_c} \right) \hat{a}^\dagger \hat{a} \right] \hat{a}^\dagger \hat{a} + \\ + \omega_1 \hat{B}_1^\dagger \hat{B}_1 + \omega_2 \hat{B}_2^\dagger \hat{B}_2. \end{aligned} \quad (14)$$

It is possible to separate the Hilbert space spanned by the Hamiltonian eigenvectors into subspaces with a definite number of photons n . The eigenstates of \hat{H}_{om} can be labelled by three indexes: the first two labelling the mechanical occupation numbers (phonons) of the two mirrors, dressed by the presence of n cavity photons while the third label describes the number n of cavity photons. We use the following notation

$$|\psi_{k,q,n}\rangle = |k_n\rangle \otimes |q_n\rangle \otimes |n\rangle_c \equiv |k, q, n\rangle. \quad (15)$$

In particular, the photon occupation number n determines the n th cavity-photon subspace, while the first two kets ($|k_n\rangle$ and $|q_n\rangle$) are the displaced mechanical Fock states, respectively, for the first and second mirror. The action of the dressed phonon operators on the eigenstates satisfy the relations

$$\begin{aligned} \hat{B}_1 |k_n, q_n, n\rangle &= \sqrt{k} |(k-1)_n, q_n, n\rangle, \\ \hat{B}_2 |k_n, q_n, n\rangle &= \sqrt{q} |k_n, (q-1)_n, n\rangle, \\ \hat{B}_1^\dagger |k_n, q_n, n\rangle &= \sqrt{(k+1)} |(k+1)_n, q_n, n\rangle, \\ \hat{B}_2^\dagger |k_n, q_n, n\rangle &= \sqrt{(q+1)} |k_n, (q+1)_n, n\rangle. \end{aligned} \quad (16)$$

The explicit expression of the single displaced Fock state $|k_n\rangle_i$ for the i th mirror is (note that from Eq. (13) and in the subspace with n cavity photons we have $B_i^\dagger = \hat{b}_i^\dagger + n\beta_i \hat{I}_i$)

$$|k_n\rangle_i = \frac{1}{\sqrt{k!}} \hat{B}_i^{\dagger k} |0_n\rangle_i = \frac{1}{\sqrt{k!}} (\hat{b}_i^\dagger + n\beta_i \hat{I}_i)^k |0_n\rangle_i, \quad (17)$$

where n -photons manifold and $|0_n\rangle_i$ is the coherent ground state for mirror i with n cavity photons, as is shown by the relation

$$\hat{b}_i |0_n\rangle_i = -n\beta_i |0_n\rangle_i, \quad (18)$$

obtained using Eq. (13) in $\hat{B}_i |0_n\rangle_i = 0$. Using the displacement operator $\hat{D}(n\beta_i) = \exp[n\beta_i(\hat{b}_i - \hat{b}_i^\dagger)]$, we have

$$|0_n\rangle_i = \hat{D}(n\beta_i) |0\rangle_i = \sum_j e^{-|n\beta_i|^2/2} \frac{(-n\beta_i)^j}{\sqrt{j!}} |j\rangle_i. \quad (19)$$

In addition, from the relation $\hat{D}(n\beta)\hat{b}^\dagger\hat{D}^\dagger(n\beta) = b^\dagger + n\beta$ [49], using Eqs. (17) and (19), we obtain

$$\begin{aligned} |k_n\rangle_i &= \frac{1}{\sqrt{k!}}(\hat{b}_i^\dagger + n\beta_i\hat{I}_i)^k|0_n\rangle_i = \\ &= \frac{1}{\sqrt{k!}}(\hat{b}_i^\dagger + n\beta_i\hat{I}_i)^k\hat{D}(n\beta_i)|0\rangle = \\ &= \hat{D}(n\beta_i)\frac{1}{\sqrt{k!}}\hat{b}_i^{\dagger k}|0\rangle = \hat{D}(n\beta_i)|k_0\rangle. \end{aligned} \quad (20)$$

Finally, after a little bit of algebra, we have

$$\begin{aligned} {}_i\langle k'_0|k_n\rangle_i &= {}_i\langle k'_0|[\hat{D}(n\beta_i)]|k_0\rangle_i = D_{k',k}(n\beta_i) = \\ &= \sqrt{k!/k'!}(n\beta_i)^{k'-k}e^{-|n\beta_i|^2/2}L_k^{k'-k}(|n\beta_i|^2), \end{aligned} \quad (21)$$

where $L_k^p(x)$ are the associated Laguerre polynomials.

In conclusion, the standard optomechanical Hamiltonian can be diagonalized as shown above and we obtain

$$\hat{H}|k, q, n\rangle = E_{k,q,n}|k, q, n\rangle, \quad (22)$$

where

$$E_{k,q,n} = \omega_c n \left[1 - \left(\frac{\beta_1^2 \omega_1}{\omega_c} + \frac{\beta_2^2 \omega_2}{\omega_c} \right) n \right] + \omega_1 k + \omega_2 q, \quad (23)$$

or, in more compact form [replacing for clarity the phonon labels as $(k, q) \rightarrow (k_1, k_2)$]

$$E_{k_1, k_2, n} = \omega_c n - \sum_i g_i^2 n^2 / \omega_i + \sum_i \omega_i k_i. \quad (24)$$

THE DCE INTERACTION HAMILTONIAN AS A PERTURBATION

In this section, we introduce the DCE interaction term. We consider this additional contribution as a perturbation to the optomechanical Hamiltonian \hat{H}_{om} . This additional term creates and destroys photon pairs. Here we consider processes at the lowest nonzero perturbation order. Thus we limit our calculations to the subspace containing zero and two cavity photons. The DCE interaction Hamiltonian \hat{V}_{DCE} is calculated using second-order perturbation theory. These perturbative calculations are carried out using the James' method [44]:

$$\hat{H}_{\text{eff}}^{(2)} = \frac{1}{i} \hat{V}_{\text{DCE}}^{I(0,2)}(t) \int_0^t V_{\text{DCE}}^{I(0,2)}(t') dt', \quad (25)$$

where

$$\hat{V}_{\text{DCE}}^{I(0,2)}(t) = e^{i\hat{H}t} \hat{V}_{\text{DCE}}^{(0,2)} e^{-i\hat{H}t}$$

is the projection operator \hat{V}_{DCE} acting in the subspace containing 0 and 2 photons expressed in the interaction

picture. After some algebra, we obtain (we assume $g_1 = g_2 \equiv g$):

$$\begin{aligned} \hat{V}_{\text{DCE}}^{I(0,2)}(t) &= \frac{g}{2} \sum_{\substack{k, q \\ k', q'}} A_{k, q}^{k', q'} |2, k_2, q_2\rangle \langle 0, k'_0, q'_0| e^{i\omega_{k, q}^{k', q'} t} + \\ &+ (A_{k, q}^{k', q'})^\dagger |0, k'_0, q'_0\rangle \langle 2, k_2, q_2| e^{-i\omega_{k, q}^{k', q'} t} \end{aligned} \quad (26)$$

where

$$\omega_{k, q}^{k', q'} = 2\Omega_c + (k' - k)\omega_1 + (q' - q)\omega_2; \quad (27)$$

with $\Omega_c = 1 + \tilde{\beta}_1 + \tilde{\beta}_2$, $\tilde{\beta}_i = g^2 / (\omega_i \omega_c)$. We also have:

$$A_{k, q}^{k', q'} = \left\langle k_2, q_2, 2 \left| \hat{V}_{\text{DCE}} \right| k'_0, q'_0, 0 \right\rangle;$$

that can be expressed in more explicit form as

$$\begin{aligned} A_{k, q}^{k', q'} &= \\ &= \sqrt{2} \left\{ [\sqrt{k'} \langle k_2 | (k' - 1)_0 \rangle + \sqrt{k' + 1} \langle k_2 | (k' + 1)_0 \rangle] \langle q_2 | q'_0 \rangle \right. \\ &\left. + [\sqrt{q'} \langle q_2 | (q' - 1)_0 \rangle + \sqrt{q' + 1} \langle q_2 | (q' + 1)_0 \rangle] \langle k_2 | k'_0 \rangle \right\}. \end{aligned} \quad (28)$$

Note that $A_{k, q}^{k', q'} = A_{k', q'}^{k, q}$. Using $D_{k', k}(2\beta_i) = \langle k'_2 | k_0 \rangle$, we have:

$$\begin{aligned} A_{k, q}^{k', q'} &= \\ &= \sqrt{2} [\sqrt{k'} D_{k, k'-1}(2\beta_1) + \sqrt{k' + 1} D_{k, k'+1}(2\beta_1)] D_{q, q'}(2\beta_2) \\ &+ \sqrt{2} [\sqrt{q'} D_{q, q'-1}(2\beta_2) + \sqrt{q' + 1} D_{q, q'+1}(2\beta_2)] D_{k, k'}(2\beta_1), \end{aligned} \quad (29)$$

where the matrix elements of the displacement operators can be expressed in terms of associated Laguerre polynomials: $D_{k', k}(\alpha) = \sqrt{k!/k'!} \alpha^{k'-k} e^{-|\alpha|^2/2} L_k^{k'-k}(|\alpha|^2)$.

One phonon – zero photons subspace

The $(1+0)$ subspace containing zero photons and one phonon excitation is spanned by the eigenvectors $|1, 0, 0\rangle$ and $|0, 1, 0\rangle$. At $\omega_2 \sim \omega_1$, these states are degenerate in absence of the \hat{V}_{DCE} interaction. In presence of such interaction, degeneracy is removed and an avoided level crossing can be observed. This effect can be described by introducing an effective Hamiltonian. Specifically: a) we introduce Eq. (26) into Eq. (25); b) we perform the integration; c) we limit the calculations to matrix elements containing zero photons; d) we transform back to the Schrödinger picture; e) finally, we project the result into the $(1+0)$ subspace spanned by the vectors $|1, 0, 0\rangle$, $|0, 1, 0\rangle$. We obtain

$$\hat{H}_{\text{eff}} = \hat{H}_{\text{eff}}^0 + [\lambda_{01}^1 |0, 1, 0\rangle \langle 1, 0, 0| + \text{H.c.}], \quad (30)$$

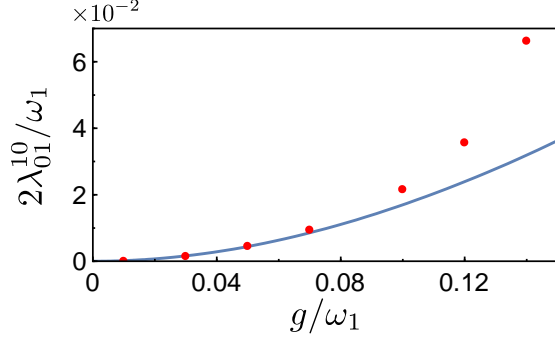


Figure 4. Comparison between the numerically calculated normalized Rabi splitting (red points) (corresponding to twice the effective coupling between the two one-phonon states $|1, 0, 0\rangle$ and $|0, 1, 0\rangle$) and the corresponding calculation using second-order perturbation theory (solid blue curve).

where

$$\hat{H}_{\text{eff}}^0 = \Omega_1 |1, 0, 0\rangle\langle 1, 0, 0| + \Omega_2 |0, 1, 0\rangle\langle 0, 1, 0|, \quad (31)$$

with $\Omega_1 = \omega_1 + \Delta_{10}$ and $\Omega_2 = \omega_2 + \Delta_{01}$, and with

$$\Delta_{10} = -\frac{g^2}{4} \sum_{kq} \frac{A_{kq}^{10\dagger} A_{kq}^{10}}{2\Omega_c + (k-1)\omega_1 + q\omega_2}; \quad (32)$$

$$\Delta_{01} = -\frac{g^2}{4} \sum_{kq} \frac{A_{kq}^{01\dagger} A_{kq}^{01}}{2\Omega_c + k\omega_1 + (q-1)\omega_2}; \quad (33)$$

$$\lambda_{01}^{10} = -\frac{g^2}{4} \sum_{kq} \frac{A_{kq}^{01\dagger} A_{kq}^{10}}{2\Omega_c + (k-1)\omega_1 + q\omega_2}. \quad (34)$$

In Fig. 4, we show a comparison between the numerically calculated normalized Rabi splitting ($2\lambda_{01}^{10}\omega_1$) between the two one-phonon states $|1, 0, 0\rangle$ and $|0, 1, 0\rangle$ and the corresponding theoretical value calculated using second-order perturbation theory as a function of the normalized optomechanical coupling g/ω_1 . The agreement is very good for g/ω_1 below 0.1.

Two phonons – zero photons subspace

The $(2+0)$ subspace with zero photons in the cavity and containing two phonon excitations is spanned by the eigenvectors: $|2, 0, 0\rangle$, $|0, 2, 0\rangle$ and $|1, 1, 0\rangle$. Also in this case, at $\omega_2 \sim \omega_1$, these states are degenerate in the absence of the \hat{V}_{DCE} interaction. With the introduction of \hat{V}_{DCE} , degeneracy is removed, and an avoided level crossing can be observed. Following the same procedure

described in the previous subsection, this effect can be described by introducing an effective Hamiltonian acting on the $(2+0)$ subspace. We obtain:

$$\hat{H}_{\text{eff}} = \hat{H}_{\text{eff}}^0 + [\lambda_{20}^{02} |2, 0, 0\rangle\langle 0, 2, 0| + \lambda_{20}^{11} |2, 0, 0\rangle\langle 1, 1, 0| + \lambda_{02}^{11} |0, 2, 0\rangle\langle 1, 1, 0| + \text{H.c.}]; \quad (35)$$

where

$$\hat{H}_{\text{eff}}^0 = \Omega_{20} |0, 2, 0\rangle\langle 0, 2, 0| + \Omega_{02} |2, 0, 0\rangle\langle 2, 0, 0| + \Omega_{11} |1, 1, 0\rangle\langle 1, 1, 0|; \quad (36)$$

with $\Omega_{20} = 2\omega_1 + \Delta_{20}$, $\Omega_{11} = \omega_1 + \omega_2 + \Delta_{11}$ and $\Omega_{02} = 2\omega_2 + \Delta_{02}$, and

$$\lambda_{20}^{02} = -\frac{g^2}{4} \sum_{kq} \frac{A_{kq}^{02\dagger} A_{kq}^{20}}{2\Omega_c + (k-2)\omega_1 + q\omega_2}, \quad (37)$$

$$\lambda_{20}^{11} = -\frac{g^2}{4} \sum_{kq} \frac{A_{kq}^{11\dagger} A_{kq}^{20}}{2\Omega_c + (k-2)\omega_1 + q\omega_2}, \quad (38)$$

$$\lambda_{02}^{11} = -\frac{g^2}{4} \sum_{kq} \frac{A_{kq}^{11\dagger} A_{kq}^{02}}{2\Omega_c + k\omega_1 + (q-2)\omega_2}, \quad (39)$$

$$\Delta_{20} = -\frac{g^2}{4} \sum_{kq} \frac{A_{kq}^{20\dagger} A_{kq}^{20}}{2\Omega_c + (k-2)\omega_1 + q\omega_2}, \quad (40)$$

$$\Delta_{02} = -\frac{g^2}{4} \sum_{kq} \frac{A_{kq}^{02\dagger} A_{kq}^{02}}{2\Omega_c + k\omega_1 + (q-2)\omega_2}, \quad (41)$$

$$\Delta_{11} = -\frac{g^2}{4} \sum_{kq} \frac{A_{kq}^{11\dagger} A_{kq}^{11}}{2\Omega_c + (k-1)\omega_1 + (q-1)\omega_2}. \quad (42)$$

A comparison of these perturbative analytical results with the numerical result is provided in the Tables I and II. The discrepancies can be ascribed to higher-order terms that at a coupling strength $g/\omega_1 = 0.1$ provide non-negligible contributions.

	$2\lambda_{01}^{10}$	$2\lambda_{20}^{11}$	$2\lambda_{20}^{02}$	$2\lambda_{02}^{11}$
Numerical \simeq	0.0217	0.0217	0.0384	0.0167
Theoretical \simeq	0.0170	0.0171	0.0348	0.0177

Table I. Comparison between the effective splittings calculated both numerically (as difference between the eigenvalues) and analytically using the James' method [44]. In particular, the theoretical values corresponding to $2\lambda_{20}^{11}$, $2\lambda_{20}^{02}$ and $2\lambda_{02}^{11}$ are obtained by the diagonalization of a 3×3 matrix representing the effective Hamiltonian in the subspace with two phonon excitations and zero photons. The cavity-mode resonance frequency is $\omega_c = 0.85\omega_1$ and $\omega_2 = \omega_1$.

	Δ_{10}	Δ_{01}	Δ_{11}	Δ_{02}	Δ_{20}
Numerical \simeq	-0.0131	-0.0159	-0.0221	-0.0239	-0.0217
Theoretical \simeq	-0.0120	-0.0121	-0.0207	-0.0199	-0.0207

Table II. Comparison between the numerically calculated energy shifts and the analytical calculations obtained using the James' method. The mechanical frequency of mirror 2 is $\omega_2 = 0.94\omega_1$. For this value the energy levels investigated do not interact significantly, and hence the energy shifts are not affected by the level-repulsion effect that occurs when the mirrors are on resonance with each other. The cavity-mode resonance frequency is $\omega_c = 0.85\omega_1$.

MECHANICAL EXCITATION TRANSFER: PULSED EXCITATION

We now investigate the transfer of mechanical excitations mediated by virtual photon pairs by exciting mirror 1 with a resonant Gaussian pulse:

$$\mathcal{F}_1(t) = \mathcal{A}\mathcal{G}(t - t_0) \cos(\omega_d t),$$

where $\omega_d = \omega_1$, and $\mathcal{G}(t)$ is a normalized Gaussian function with standard deviation $\sigma = 1/(10\lambda_{10}^{01})$. We consider the case of the strong coupling regime, when the mirror-mirror coupling strength λ_{10}^{01} is larger than the total decoherence rate $\gamma_1 + \gamma_2$. We set the resonance frequency of mirror 2 to $\omega_2 \simeq \omega_1$ providing the minimum level splitting $2\lambda_{10}^{01}$. The system starts in its ground state. Figure 5 displays the system dynamics after the pulse arrival and the Fourier transform of the mean phonon number of mirror 1 (no relevant changes occur for mirror 2), obtained for pulses with amplitudes increasing from top to bottom: $\mathcal{A} = 0.25\pi, 0.45\pi$. Panels 5(a) and 5(α) have been obtained using the loss rates $\gamma = 3.5 \times 10^{-3}\omega_1$ and $\kappa = 0.5\gamma$. Figure 5(a) displays coherent and reversible sinusoidal oscillations (with peak amplitudes decaying exponentially), showing that the mechanical state of the spatially separated mirrors is transferred from one to the other at a rate $\omega_{3,2} \equiv E_3 - E_2 = \lambda_{10}^{01}$, as confirmed by the peak in the Fourier transform in Fig. 5(α). We notice that the position and broadening of the peak at $\omega_{3,2}$ in Fig. 5(α) is influenced by the initial dynamics of $\langle \hat{B}_1^\dagger \hat{B}_1 \rangle$, which in turn is affected by the pulse shape (Fig. 6 displays the corresponding spectrum for mirror 2). The higher peak at $\omega = 0$ originates from the exponential decay of the signal. These results clearly show that, for the weaker excitation amplitude ($\mathcal{A} = 0.25\pi$), only the one-phonon states $|1, 0, 0\rangle$ and $|0, 1, 0\rangle$ are excited significantly and contribute to the dynamics.

By increasing the pulse amplitude [Fig. 5(b)], the mean phonon numbers grow significantly and the signals are no more sinusoidal, owing to the additional excitation of the states $|2, 0, 0\rangle$, $|1, 1, 0\rangle$, and $|0, 2, 0\rangle$, whose DCE-induced coupling gives rise to the hybridized energy eigenstates $|\psi_7\rangle$, $|\psi_8\rangle$, and $|\psi_9\rangle$. In order to better distinguish the nonsinusoidal behaviour, we used much lower loss rates: $\gamma = 8 \times 10^{-5}\omega$ and $\kappa = 0.5\gamma$. Figure 5(β) shows the appearance of an additional peak at $\omega = \omega_{8,7}$, confirming that higher-energy mechanical states get excited. We ob-

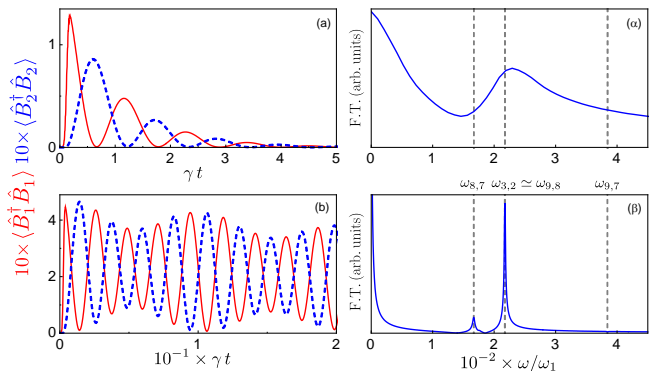


Figure 5. Time evolution of the mean phonon numbers of the two mirrors after the arrival of the pulse. We consider two different amplitudes which increase from top to bottom: $\mathcal{A} = 0.25\pi$ (a), 0.45π (b). Specifically, panels (a-b) display the mean phonon numbers $\langle \hat{B}_i^\dagger \hat{B}_i \rangle$. Panels (α - β) display the Fourier transform of the mean phonon number shown in the corresponding panel on the left. Other parameters are given in the text.

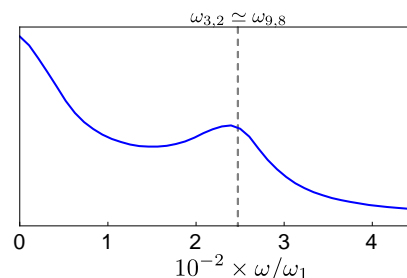


Figure 6. Fourier transform of the mean phonon number of mirror 2 obtained for a pulse with amplitude $\mathcal{A} = 0.25\pi$.

serve that the frequency splitting $\omega_{9,8}$ is very close to $\omega_{3,2}$, hence, it does not give rise to a new peak in Fig. 5(β). Moreover, the frequency splitting at $\omega_{9,7}$ does not contribute significantly to the dynamics as confirmed by the spectrum in Fig. 5(β). An analytic calculation based on three coupled levels confirms that the used parameters give rise to a negligible contribution at $\omega_{9,7}$.

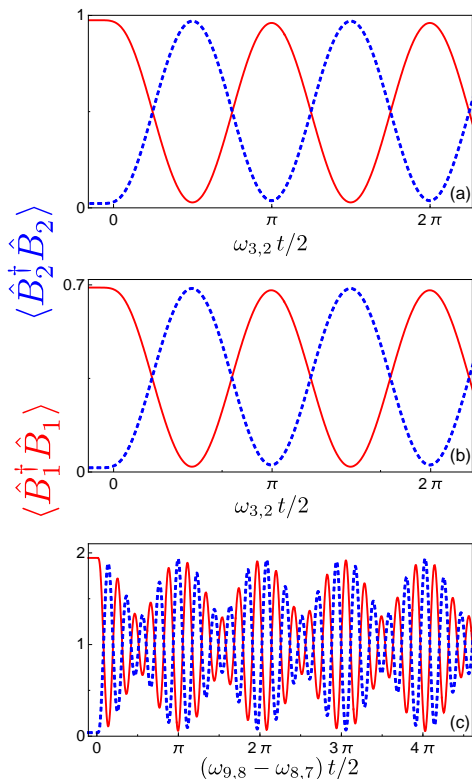


Figure 7. Time evolution of the mean phonon numbers of the two mirrors obtained preparing the system in an initial state (a) $|1, 0, 0\rangle$, (b) $\frac{1}{\sqrt{2}}(|1, 0, 0\rangle + |0, 0, 1\rangle)$, (c) $|2, 0, 0\rangle$. Mirror 2 is initially set at a mechanical frequency ω_2^{in} (details are given in the text). We note that the dynamics display oscillations, (a) and (b), due to the avoided level crossing between the states $|\psi_3\rangle$ and $|\psi_2\rangle$ with frequency equal to $\omega_{3,2}$; (c) due to the splittings between the states $|\psi_9\rangle$, $|\psi_8\rangle$ and $|\psi_7\rangle$, whose transitions from higher to lower levels give rise to beats (the details are given in the text).

MECHANICAL EXCITATION TRANSFER: NONADIABATIC EFFECTIVE SWITCHING OF THE INTERACTION

As pointed out in the last paragraph of the main paper, if it is possible to control the interaction time (as currently realized in superconducting artificial atoms), e.g., by rapidly changing the resonance frequencies of the mechanical oscillators, the interaction scheme proposed here would represent an attractive architecture for quantum information processing with optomechanical systems. Here we provide some examples of quantum state transfer. In Fig. 7, we show the phonon population dynamics obtained preparing the system in three different initial states (a) $|1, 0, 0\rangle$, (b) $\frac{1}{\sqrt{2}}(|0, 0, 0\rangle + |1, 0, 0\rangle)$, (c) $|2, 0, 0\rangle$. Mirror 2 is initially set at a mechanical frequency ω_2^{in} . This value must be chosen sufficiently far from the value $\omega_2^{\text{min}} \simeq 0.99\omega_1$ corresponding to the minimum splitting

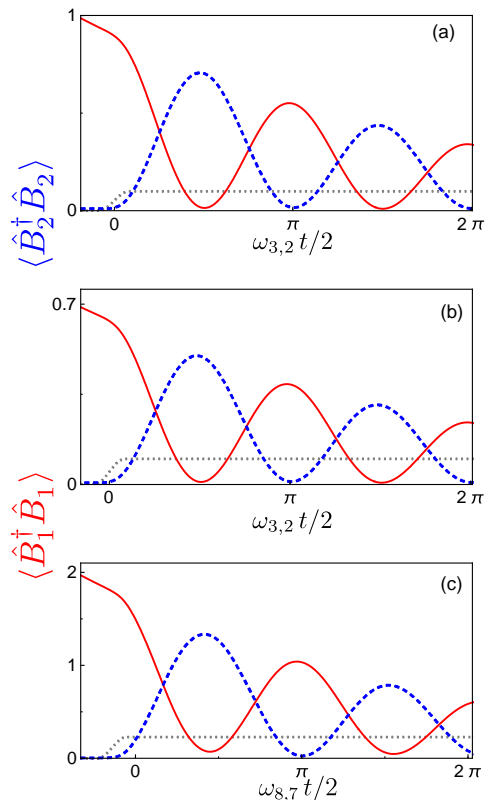


Figure 8. Time evolution of the mean phonon numbers of the two mirrors calculated after a non-adiabatic switching of the interaction, as explained in Fig. 7, but in the presence of losses both in mirrors and cavity. The parameters are the same as in Fig. 7; in addition we have $\gamma = \gamma_1 = \gamma_2 = \omega_1/650$ and $\kappa = 0.5\gamma$. The system is initially prepared in the states (a) $|1, 0, 0\rangle$, (b) $\frac{1}{\sqrt{2}}(|1, 0, 0\rangle + |0, 0, 1\rangle)$, (c) $|2, 0, 0\rangle$. As we can observe, the oscillations are damped and disappear after a few periods. In (c) the losses do not allow for observations of beats oscillations having a longer time period. The dotted gray lines show how the frequency of mirror 2 is tuned into resonance with mirror 1 (details are given in the text).

between states $|1, 0, 0\rangle$ and $|0, 1, 0\rangle$. In particular, we have fixed $\omega_2^{\text{in}} = \omega_2^{\text{min}} - \delta$ with $\delta = 0.069\omega_1$. This value is also sufficiently far from the region where the avoided three-level crossing between the states $|\psi_i\rangle$ with $i = 7, 8, 9$ appears. Subsequently, a time-dependent perturbation $H_{\text{na}} = f(t)\hat{B}_2^\dagger\hat{B}_2$ [with $f(t) \approx \theta(t - t_0)$] is introduced in order to modify the resonance frequency of mirror 2 (θ is the Heaviside step function). More specifically $f(t) = \delta [\sin^2[\Omega(t - t_0)\theta(t - t_0) + \sin^2[\Omega(t - t_f)\theta(t - t_f)]]$ is a smoothed step function, where δ fixes the change in mechanical frequency of mirror 2, t_0 is the time when the frequency starts to change, $t_f = t_0 + \pi/(2A)$, and Ω is the frequency setting the smoothness.

This enables a non-adiabatic transition from the frequency region with $\omega_2 = \omega_2^{\text{in}}$, where the states $|2, 0, 0\rangle$, $|1, 0, 0\rangle$ and $|0, 1, 0\rangle$ are eigenstates of the system, to the frequency region $\omega_2 = \omega_2^{\text{min}}$ where the former states are

no longer eigenstates of the system. As a consequence, the dynamics of the phonon populations of the two mirrors display *quantum Rabi-like* oscillations [see Fig. 7(a) and (b)] due to the avoided level crossing between the states $|\psi_3\rangle$ and $|\psi_2\rangle$ (the eigenstates of the systems are, in this frequency region, the symmetric and antisymmetric superpositions of $|1, 0, 0\rangle$ and $|0, 1, 0\rangle$; see Fig. 1b in the main paper). In Fig. 7(c), the avoided level crossing between the states $|\psi_9\rangle$, $|\psi_8\rangle$, and $|\psi_7\rangle$ gives rise to transitions from higher to lower levels. As a consequence, we observe beats between the two transition frequencies $\omega_{8,9}$ and $\omega_{8,7}$ (with the chosen parameters the other frequency transition $\omega_{9,7}$ does not contribute to the beats). Finally, in Fig. 8, we show the time evolution of the mean phonon numbers for the same cases discussed above, but in the presence of losses both in mirrors and cavity. We observe the damping of the population dynamics as expected in presence of losses.

FN was partially supported by the MURI Center for Dynamic Magneto-Optics via the AFOSR Award No. FA9550-14-1-0040, the Japan Society for the Promotion of Science (KAKENHI), the IMPACT program of JST, JSPS-RFBR grant No 17-52-50023, CREST grant No. JPMJCR1676, RIKEN-AIST Challenge Research Fund, and the Sir John Templeton Foundation. AFK acknowledges support from a JSPS Postdoctoral Fellowship for Overseas Researchers (P15750).

* corresponding author: ssavasta@unime.it

- [1] J. Majer, J. M. Chow, J. M. Gambetta, J. Koch, B. R. Johnson, J. A. Schreier, L. Frunzio, D. I. Schuster, A. A. Houck, A. Wallraff, A. Blais, M. H. Devoret, S. M. Girvin, and R. J. Schoelkopf, "Coupling superconducting qubits via a cavity bus," *Nature* **449**, 443 (2007).
- [2] A. Sørensen and K. Mølmer, "Quantum computation with ions in thermal motion," *Phys. Rev. Lett.* **82**, 1971 (1999).
- [3] A. Imamoglu, D. D. Awschalom, G. Burkard, D. P. DiVincenzo, D. Loss, M. Sherwin, and A. Small, "Quantum information processing using quantum dot spins and cavity QED," *Phys. Rev. Lett.* **83**, 4204 (1999).
- [4] S.-B. Zheng and G.-C. Guo, "Efficient scheme for two-atom entanglement and quantum information processing in cavity QED," *Phys. Rev. Lett.* **85**, 2392 (2000).
- [5] S. Osnaghi, P. Bertet, A. Auffeves, P. Maioli, M. Brune, J.-M. Raimond, and S. Haroche, "Coherent control of an atomic collision in a cavity," *Phys. Rev. Lett.* **87**, 037902 (2001).
- [6] S. Filipp, M. Göppl, J. M. Fink, M. Baur, R. Bianchetti, L. Steffen, and A. Wallraff, "Multimode mediated qubit-qubit coupling and dark-state symmetries in circuit quantum electrodynamics," *Physical Review A* **83**, 063827 (2011).
- [7] L. DiCarlo, J. M. Chow, J. M. Gambetta, L. S. Bishop, B. R. Johnson, D. I. Schuster, J. Majer, A. Blais, L. Frunzio, S. M. Girvin, and R. J. Schoelkopf, "Demonstration of two-qubit algorithms with a superconducting quantum processor," *Nature* **460**, 240 (2009).
- [8] M. Neeley, R. C. Bialczak, M. Lenander, E. Lucero, M. Mariantoni, A. D. O'Connell, D. Sank, H. Wang, M. Weides, J. Wenner, Y. Yin, T. Yamamoto, A. N. Cleland, and J. M. Martinis, "Generation of three-qubit entangled states using superconducting phase qubits," *Nature* **467**, 570 (2010).
- [9] R. Stassi, V. Macrì, A. F. Kockum, O. Di Stefano, A. Miranowicz, S. Savasta, and F. Nori, "Quantum nonlinear optics without photons," *Phys. Rev. A* **96**, 023818 (2017).
- [10] P. Zhao, X. Tan, H. Yu, S.-L. Zhu, and Y. Yu, "Circuit QED with qutrits: Coupling three or more atoms via virtual-photon exchange," *Phys. Rev. A* **96**, 043833 (2017).
- [11] A. F. Kockum, A. Miranowicz, V. Macrì, S. Savasta, and F. Nori, "Deterministic quantum nonlinear optics with single atoms and virtual photons," *Phys. Rev. A* **95**, 063849 (2017).
- [12] A. F. Kockum, V. Macrì, L. Garziano, S. Savasta, and F. Nori, "Frequency conversion in ultrastrong cavity QED," *Sci. Rep.* **7**, 5313 (2017).
- [13] C. A. Sackett, D. Kielpinski, B. E. King, C. Langer, V. V. Meyer, C. J. Myatt, M. Rowe, Q. A. Turchette, W. M. Itano, D. J. Wineland, and C. Monroe, "Experimental entanglement of four particles," *Nature* **404**, 256 (2000).
- [14] D. Leibfried, B. DeMarco, V. Meyer, D. Lucas, M. Barrett, J. Britton, W. M. Itano, B. Jelenković, C. Langer, T. Rosenband, and D. J. Wineland, "Experimental demonstration of a robust, high-fidelity geometric two ion-qubit phase gate," *Nature* **422**, 412 (2003).
- [15] M. Kardar and R. Golestanian, "The "friction" of vacuum, and other fluctuation-induced forces," *Rev. Mod. Phys.* **71**, 1233 (1999).
- [16] D. A. R. Dalvit and P. A. Maia Neto, "Decoherence via the dynamical Casimir effect," *Phys. Rev. Lett.* **84**, 798 (2000).
- [17] M. T. Jackel and S. Reynaud, "Fluctuations and dissipation for a mirror in vacuum," *Quantum Opt.* **4**, 39 (1992).
- [18] M. T. Jackel and S. Reynaud, "Motional Casimir force," *J. Phys. I* **2**, 149 (1992).
- [19] A. D. O'Connell, M. Hofheinz, M. Ansmann, R. C. Bialczak, M. Lenander, E. Lucero, M. Neeley, D. Sank, H. Wang, M. Weides, *et al.*, "Quantum ground state and single-phonon control of a mechanical resonator," *Nature* **464**, 697 (2010).
- [20] F. Rouxinol, Y. Hao, F. Brito, A. O. Caldeira, E. K. Irish, and M. D. LaHaye, "Measurements of nanoresonator-qubit interactions in a hybrid quantum electromechanical system," *Nanotechnology* **27**, 364003 (2016).
- [21] C. F. Ockeloen-Korppi, E. Damskagg, J. M. Pirkkalainen, A. A. Clerk, F. Massel, M. J. Woolley, and M. A. Sillanpää, "Entangled massive mechanical oscillators," [arXiv:1711.01640](https://arxiv.org/abs/1711.01640) (2017).
- [22] C. K. Law, "Interaction between a moving mirror and radiation pressure: A Hamiltonian formulation," *Phys. Rev. A* **51**, 2537 (1995).
- [23] V. Macrì, A. Ridolfo, O. Di Stefano, A. F. Kockum, F. Nori, and S. Savasta, "Non-perturbative dynamical Casimir effect in optomechanical systems: Vacuum Casimir-Rabi splittings," [arXiv:1706.04134](https://arxiv.org/abs/1706.04134) (2017).
- [24] K. Sala and T. Tufarelli, "Exploring corrections to the optomechanical Hamiltonian," [arXiv:1711.06688](https://arxiv.org/abs/1711.06688) (2017).
- [25] M. Aspelmeyer, T. J. Kippenberg, and F. Marquardt,

- “Cavity optomechanics,” *Rev. Mod. Phys.* **86**, 1391 (2014).
- [26] G. T. Moore, “Quantum Theory of the Electromagnetic Field in a Variable-Length One-Dimensional Cavity,” *J. Math. Phys.* **11**, 2679 (1970).
- [27] P. D. Nation, J. R. Johansson, M. P. Blencowe, and Franco Nori, “Colloquium: Stimulating uncertainty: Amplifying the quantum vacuum with superconducting circuits,” *Rev. Mod. Phys.* **84**, 1–24 (2012).
- [28] J. R. Johansson, G. Johansson, C. M. Wilson, and F. Nori, “Dynamical Casimir Effect in a Superconducting Coplanar Waveguide,” *Phys. Rev. Lett.* **103**, 147003 (2009).
- [29] J. R. Johansson, G. Johansson, C. M. Wilson, and F. Nori, “Dynamical Casimir effect in superconducting microwave circuits,” *Phys. Rev. A* **82**, 52509 (2010).
- [30] C. M. Wilson, G. Johansson, A. Pourkabirian, M. Simoen, J. R. Johansson, T. Duty, F. Nori, and P. Delsing, “Observation of the dynamical Casimir effect in a superconducting circuit,” *Nature* **479**, 376 (2011).
- [31] J. R. Johansson, G. Johansson, C. M. Wilson, P. Delsing, and F. Nori, “Nonclassical microwave radiation from the dynamical Casimir effect,” *Phys. Rev. A* **87**, 043804 (2013).
- [32] S. Felicetti, M. Sanz, L. Lamata, G. Romero, G. Johansson, P. Delsing, and E. Solano, “Dynamical Casimir effect entangles artificial atoms,” *Phys. Rev. Lett.* **113**, 093602 (2014).
- [33] R. Stassi, S. De Liberato, L. Garziano, B. Spagnolo, and S. Savasta, “Quantum control and long-range quantum correlations in dynamical Casimir arrays,” *Phys. Rev. A* **92**, 013830 (2015).
- [34] D. Z. Rossatto, S. Felicetti, H. Eneriz, E. Rico, M. Sanz, and E. Solano, “Entangling polaritons via dynamical Casimir effect in circuit quantum electrodynamics,” *Phys. Rev. B* **93**, 094514 (2016).
- [35] T. T. Heikkilä, F. Massel, J. Tuorila, R. Khan, and M. A. Sillanpää, “Enhancing optomechanical coupling via the Josephson effect,” *Phys. Rev. Lett.* **112**, 203603 (2014).
- [36] F. Beaudoin, J. M. Gambetta, and A. Blais, “Dissipation and ultrastrong coupling in circuit QED,” *Phys. Rev. A* **84**, 043832 (2011).
- [37] D. Hu, S.-Y. Huang, J.-Q. Liao, L. Tian, and H.-S. Goan, “Quantum coherence in ultrastrong optomechanics,” *Phys. Rev. A* **91**, 013812 (2015).
- [38] H.-P. Breuer and F. Petruccione, *The Theory of Open Quantum Systems* (Oxford University Press, 2002).
- [39] K. K. W. Ma and C. K. Law, “Three-photon resonance and adiabatic passage in the large-detuning Rabi model,” *Phys. Rev. A* **92**, 023842 (2015).
- [40] L. Garziano, R. Stassi, V. Macrì, S. Savasta, and O. Di Stefano, “Single-step arbitrary control of mechanical quantum states in ultrastrong optomechanics,” *Phys. Rev. A* **91**, 023809 (2015).
- [41] V. Macrì, L. Garziano, A. Ridolfo, O. Di Stefano, and S. Savasta, “Deterministic synthesis of mechanical NOON states in ultrastrong optomechanics,” *Phys. Rev. A* **94**, 013817 (2016).
- [42] See Supplemental Material for more details.
- [43] O. Gamel and D. F. V. James, “Time-averaged quantum dynamics and the validity of the effective Hamiltonian model,” *Phys. Rev. A* **82**, 052106 (2010).
- [44] W. Shao, C. Wu, and X.-L. Feng, “Generalized James’ effective Hamiltonian method,” *Phys. Rev. A* **95**, 032124 (2017).
- [45] A. Ridolfo, M. Leib, S. Savasta, and M. J. Hartmann, “Photon Blockade in the Ultrastrong Coupling Regime,” *Phys. Rev. Lett.* **109**, 193602 (2012).
- [46] L. Garziano, R. Stassi, V. Macrì, A. F. Kockum, S. Savasta, and F. Nori, “Multiphoton quantum Rabi oscillations in ultrastrong cavity QED,” *Phys. Rev. A* **92**, 063830 (2015).
- [47] L. Garziano, R. Stassi, V. Macrì, O. Di Stefano, F. Nori, and S. Savasta, “One Photon Can Simultaneously Excite Two or More Atoms,” *Phys. Rev. Lett.* **117**, 043601 (2016).
- [48] K. Stannigel, P. Komar, S. J. M. Habraken, S. D. Bennett, M. D. Lukin, P. Zoller, and P. Rabl, “Optomechanical quantum information processing with photons and phonons,” *Phys. Rev. Lett.* **109**, 013603 (2012).
- [49] M. O. Scully and M. S. Zubairy, *Quantum Optics* (Cambridge University Press, 1997).